MULTI-AXIS LONG-DURATION BLAST INTERACTION WITH I-SHAPE STEEL SECTIONS

J.W. Denny, S.K. Clubley

Blast Damage and Weapons Effects Research Team, Faculty of Engineering and the Environment, University of Southampton, Southampton, Hampshire, SO17 1BJ, UK

ABSTRACT

Accurate characterisation of blast loading on intricate structural components is a challenging task. This paper reports experimental results pertaining to the effects of planar long-duration blast waves interacting with exposed I-shape steel sections about multiple axes. Long-duration blasts are defined by a positive phase duration t^+>100ms, characteristic of very large explosion events in the far field. These can result in significantly large impulses and dynamic pressures. Multi-axis long-duration blast interaction with intricate I-sections gives rise to rapid blast diffraction and translational drag loading effects which are complex to characterise, generally requiring approximation using crude drag coefficients. Blast drag coefficients available in literature lack provision for multi-axis interaction with I-shape geometries. Four full-scale long-duration blast experiments investigate the blast interaction with an I-shape column as a function of section orientation with respect to the incident shock wave. High-fidelity pressure instrumentation record coupled incident and reflected surface blast parameters. It was found that constituent surface specific impulse varied with section orientation due to relative exposure to the blast and local shielding aerodynamic effects. Results demonstrate that I-section orientation with respect to blast propagation has significant influence on the resultant translational loading. Experimental drag force coefficients as a function of section orientation are calculated from experimental data and compared to values proposed in literature providing conclusions of direct relevance to both design practitioners and academics.

INTRODUCTION

Long-duration blast pressures, defined by a positive phase duration t^+>100ms, are characteristic of very large explosions, with examples including nuclear detonations and industrial chemical storage accidents including hydrocarbon vapour cloud explosions. Recent examples of such events include the 'Buncefield Disaster'(2005) [1], the 'Texas Fertiliser Plant Disaster' (2013) and the Tianjin industrial accident (2015). These explosions generate substantial impulse and dynamic pressures, considerably exceeding shorter duration blasts with the same peak overpressures. Steel column sections are found extensively in the construction of single to multi-storey framed structures. Analysing blast loading effects of such members is of interest due to increased security demands and the prevalence of large-scale industrial accidents involving destructive blasts with long-duration characteristics.

Accurate characterisation of multi-axis blast loading on exposed I-sections is a challenging task. Due to rapid blast diffraction and 'equalisation' of overpressures, slender I-sections are 'drag targets', predominantly affected by translational loading associated with blast drag pressures. Column geometry and section orientation with respect to the blast (multi-axis interaction) gives rise to varying magnitudes of translational drag loading. Much contemporary research has focused on analysing the effects of short-duration, impulsive blast loads on column sections where drag loading effects are minimal. Furthermore, previous research [2][3] on structural response to long-duration blasts generally assume infinite surfaces which, in the case of exposed I-sections that exhibit a high degree of 'finiteness', is not appropriate [4]. Given the complex nature of structural blast interaction, and in particular for drag targets such as exposed columns, engineers tend to

simplify the problem by employing drag coefficients to predict the net translational blast loading [2], [5]–[7]. However, very few proposed drag coefficients exist in available literature or design manuals for specific column section geometries that are suitable or verified for application to long-duration blast loading. Proposed drag coefficients are generally single values which only consider blast interaction about a single orthogonal axis, thus lacking provision for multi-axis interaction or different 'angles of attack'. Drag loading effects for oblique, intermediate section orientations is therefore unknown, greatly limiting the accuracy of predicting blast loading on exposed column elements when multi-axis behaviour is concerned.

The main objective of this paper is to present new experimental findings relating to the blast air flow around steel I-sections and quantify the forces imparted as a function of section orientation. Based on experimental results, net impulses experienced by an I-section column aligned at different orientations to the blast are quantified and used to derive drag force coefficients. In the absence of appropriate or verified blast drag coefficients for I-sections at oblique orientations, these experiments provide an insight to the multi-axis effects when long-duration blast drag loading is predominant. The effect of multi-axis interaction of I-sections subjected to long-duration blast loading and the associated drag force coefficients was previously unknown. This paper provides experimental results to inform the engineer towards more accurate calculation of blast loads and selection of drag coefficients for an I-section subjected to blast loading about different axes.

EXPERIMENTAL METHODOLOGY

Four full-scale long-duration blast experiments were conducted to investigate and quantify the effects of multi-axis blast loading on a steel I-section column. Long-duration, planar blast waves were generated using the Air Blast Tunnel (ABT) facility at MoD Shoeburyness, UK, one of very few facilities in the world capable of examining the structural response to long-duration blast loads (Figure 1). The ABT is capable of generating blast waves with 'long duration' characteristics; a positive phase duration of $t^+ \approx 155$ms is achievable at maximum power, differing greatly in comparison to the shorter durations of 10-20ms, typical of conventional arena blast experiments. For each experiment, blast waves with consistent parameters were sought: a peak overpressure, p_i=55kPa, a positive phase duration, t^+=155ms and a total free-field impulse of I_i=3380kPa.ms.

Figure 1: The Air Blast Tunnel (ABT), MOD Shoeburyness, UK.

Multi-axis blast loading was investigated by aligning a 3.00m UKC 203x203x46 I-section column at four orientations to the incident shock wave. Repeat blast loading (a total of four firings) examined four section orientations of 0, 30, 60 and 90 degrees (Figure 2). The column was fixed at the base inside the ABT in a cantilever configuration utilising a bespoke, adjustable base plate design which enabled the section to be rotated in-situ to achieve the required orientations (Figure 3). The section was designed to respond elastically to the blast loading to permit repeat firings about different orientations without causing plastic deformation.

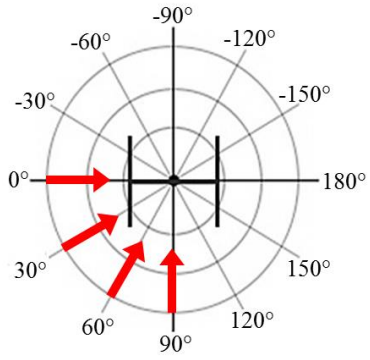

Figure 2 (top right): Multi-axis blast angle convention adopted for experiments (red arrows indicate the axes explored in the experiments).

Figure 3: Photographs of the column specimen and baseplate at the 30° orientation.

Each experiment sought to accurately quantify column blast pressure interaction for the section orientations tested. This was accomplished by instrumenting the column with 8 Endevco 8515C-50 pressure transducers secured to the centre point of each cross-section surface at mid-height, numbered 1-8 as illustrated in Figure 4. Pressure transducers recorded the blast flow field interaction and respective surface pressure histories for each orientation examined. Incident blast environment data was captured by instrumenting a location precisely 2.00m adjacent to the column assembly. Endevco 8510-50 static overpressure transducers and Kulite-20D dynamic pressure gauges enabled measurement of peak pressures, specific impulse and positive phase durations for the free-field blast environment.

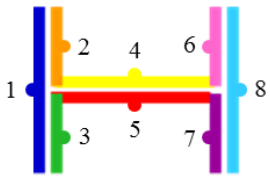

Figure 4: Surface pressure transducer numbering convention (1-8).

EXPERIMENTAL RESULTS & DISCUSSION

High-fidelity pressure data was analysed to quantify the incident and I-section surface blast parameters, thus enabling calculation of the net translational loading for each orientation examined. Consistent static overpressure-time histories, and the associated cumulative specific impulse were observed in each experiment demonstrating an ideal blast wave type i.e. a Friedlander decay curve (Figure 5). Similarly, time histories of dynamic pressure and associated cumulative impulse were approximately consistent for the four experiments (Figure 5).

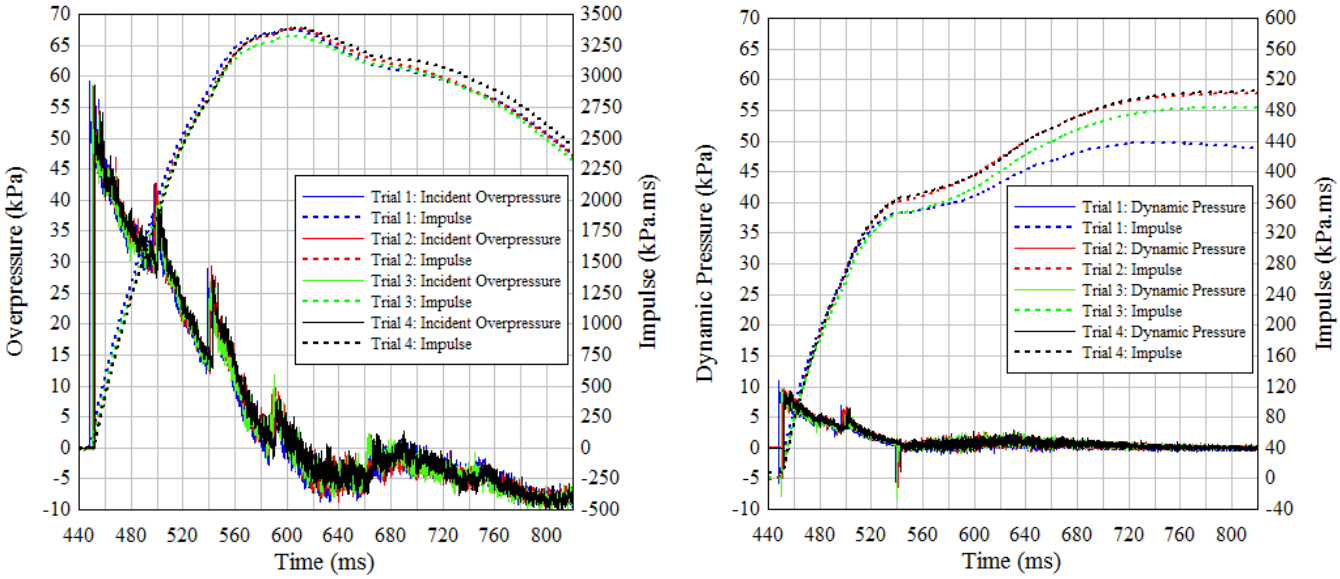

Figure 5: Incident static overpressure (left) and dynamic pressure (right) time histories and cumulative impulse.

For the four experiments, an average peak incident static overpressure of p_i=58.7kPa, positive phase duration of 154.3ms and a mean incident impulse of 3369.7kPa.ms was recorded (Table 1). A mean peak dynamic pressure and associated impulse of 60.0kPa and 463.0kPa.ms respectively were recorded for all experiments (Table 2).

Table 1: Incident blast environment - static overpressure.

Experimental Data Incident Overpressure Parameters	Trial 1	Trial 2	Trial 3	Trial 4	Mean
Peak incident overpressure (kPa)	59.1	58.4	58.6	58.5	58.7
Positive phase duration (ms)	154.2	154.8	152.6	155.6	154.3
Positive phase incident impulse (kPa.ms)	3377.3	3386.6	3326.5	3388.5	3369.7

Table 2: Incident blast environment - dynamic pressure.

Experimental Data Incident Dynamic Pressure Parameters	Trial 1	Trial 2	Trial 3	Trial 4	Mean
Dynamic pressure (kPa)	10.9	9.7	9.6	9.4	9.9
Positive phase duration (ms)	286.1	337.2	305.9	339.0	296.0
Positive phase dynamic impulse (kPa.ms)	437.8	484.4	449.8	480.0	463.0

For each experiment, 8 transducers recorded surface pressure-time histories on respective surfaces of the I-section. Surface impulses were calculated by integrating the reflected overpressure-time histories for the positive phase duration (Table 3). Unlike peak reflected pressure values, surface impulse relates to the entire pressure-time profile recorded at a particular surface. Specific impulse values quantify the overall blast energy transferred to surfaces of the column when stagnation drag pressures are the predominant loading mechanism. Calculated total surface impulse variation with section orientation is plotted and tabulated in Figure 6 and Table 3 respectively.

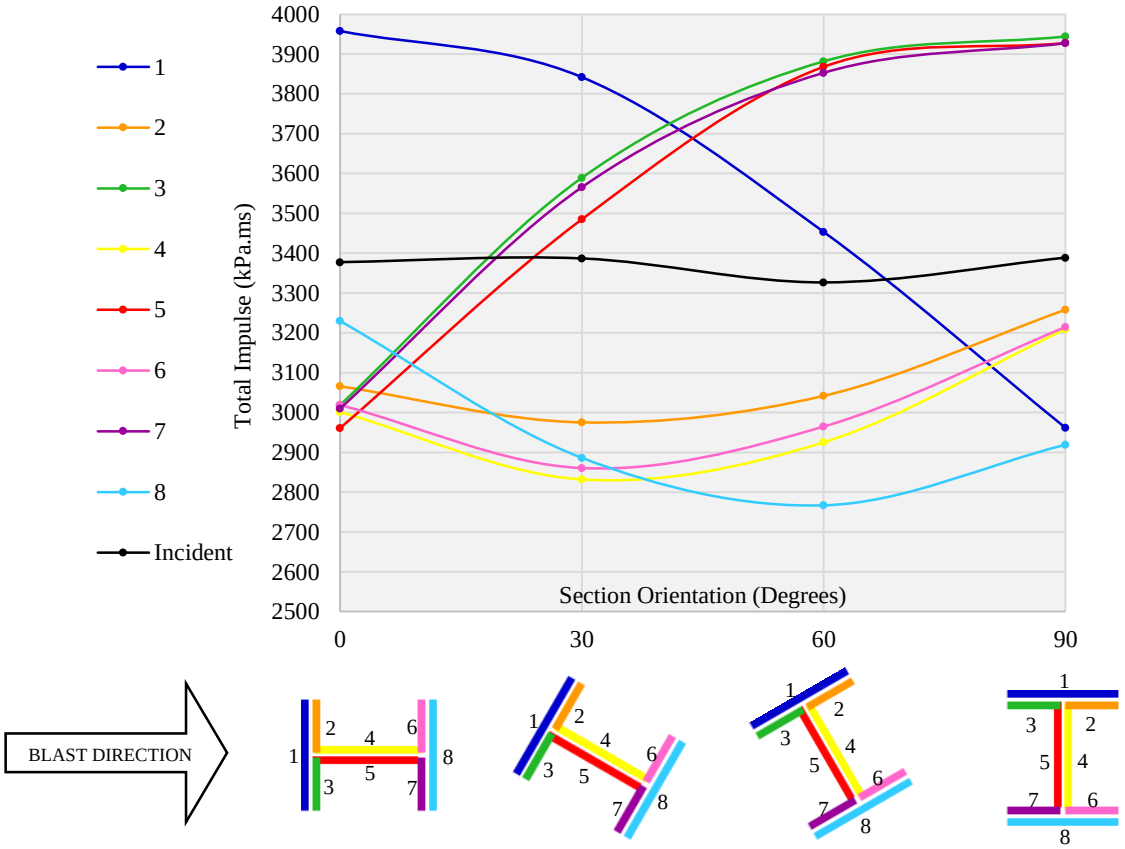

Figure 6: Surface total impulse variation with I-section orientation.

Table 3: Total impulse recorded at each surface for different I-section orientations.

Trial	Section Orientation	Experimental Data: Surface Total Impulse Values (kPa.ms)								
		Incident	1	2	3	4	5	6	7	8
1	0°	3377	3958	3070	3019	3001	2961	3019	3010	3230
2	30°	3387	3842	2975	3589	2832	3485	2861	3566	2886
3	60°	3327	3454	3042	3882	2925	3868	2965	3853	2767
4	90°	3389	2961	3258	3944	3209	3928	3215	3927	2919

Total impulses on the I-section surfaces vary considerably with orientation to the blast (Figure 6). This variation can be attributed to both the relative exposure of a particular surface to the blast and the presence of aerodynamic effects. Exposed surfaces exhibited the highest impulses; a maximum impulse was observed for the front flange (surface 1) at the 0° orientation and surfaces 3, 5 and 7 at the 90° orientation for example (Figure 6). In these cases, exposed surfaces experience a total impulse exceeding the free-field incident impulse (Figure 6). For less exposed or ‘shielded’

surfaces, total surface impulses fall below the free-field value (Figure 6). Surfaces 2, 4, 6 and 8 are comparably shielded from the blast throughout orientations 0°-90° with total impulse values consistently below that of the incident blast wave (Figure 6). Collectively, these four shielded surfaces experience minimum impulse for the 30° orientation (Figure 6), approximately ≈500kPa.ms less than the free-field value. This indicates a high degree of shielding where aerodynamic effects such as flow separation manifest as reduced stagnation pressures on these surfaces. As the section is rotated to 60°, the rear flange (surface 8) impulse continues to decrease to a minimum value whilst the shielded surfaces (2, 4 and 6) impulse gradually increases indicating that the shielding effects become less prominent. Of note, a minimum impulse value for surface 8 occurs for the 60° orientation, thus indicating a high degree of shielding from the blast. At the 90° orientation surface 2, 4 and 6 impulses continue to increase to the order of 3210-3260 kPa.ms, comparable to the incident impulse (3389kPa.ms). These relatively higher impulse values recorded for these surfaces demonstrate that despite being directly unexposed to the blast, shielding aerodynamic effects are reduced for this orientation. This enables larger stagnation pressures to establish on these rear surfaces, hence relatively higher impulse values. As a result, respective surface impulses are affected by both relative exposure to the blast wave and the aerodynamic interaction with the section geometry features.

To quantify the overall translational load acting on the column as a function of section orientation, the net total impulse is calculated for the I-section orthogonal axes, x', y' and the corresponding resultant impulse vector, R' as illustrated in Figure 7. Calculated net component impulse vectors for each section orientation are plotted in Figure 8.

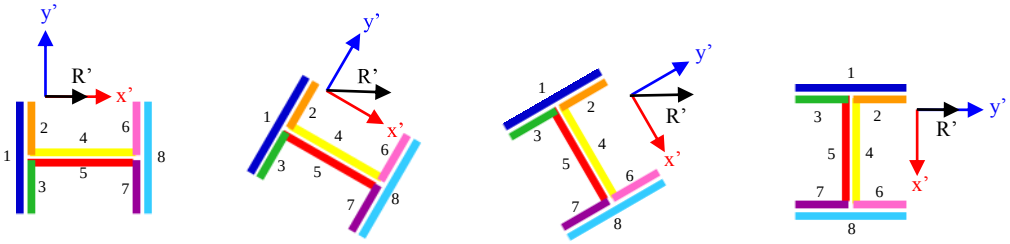

Figure 7: Net impulse vector components for varying section orientation: $I_{x'}$, $I_{y'}$ and $I_{R'}$.

Both orthogonal orientations exhibit similar net resultant impulses of 702 kPa.ms and 719 kPa.ms for the 0° and 90° orientations respectively. For intermediate orientations however, varying magnitudes of net impulse components, x' and y' exist. The 30° orientation results in a larger net x' impulse than for the 0° orientation (Figure 8). This can be explained by interior flange surfaces having greater exposure, causing a larger x' impulse effect. Also at the 30° orientation, the web surface becomes exposed causing the net y' impulse to increase, producing a resultant net impulse R'=1102 kPa.ms, a 57% increase from the 0° orientation. Similarly, the 60° orientation results in a larger net y' impulse than at the 90° orientation. This can be attributed to the reduced restoring impulse established on the rear surfaces due to a high degree of aerodynamic shielding. The geometry features at this orientation cause the rear web (surface 4) to attain a much lower impulse than the exposed web surface (5), thus a relatively large net y' impulse. The 60° orientation results in the largest net impulse of the four orientations investigated with a resultant impulse R'=1136 kPa.ms; this is approximately 62% higher than the 0° orientation and 58% higher than that of the 90° orientation. This confirms that multi-axis blast interaction with I-sections can result in larger magnitude loading effects. Inspection of Figure 8 implies a maximum resultant impulse occurs at an intermediate orientation between 30° and 60°.

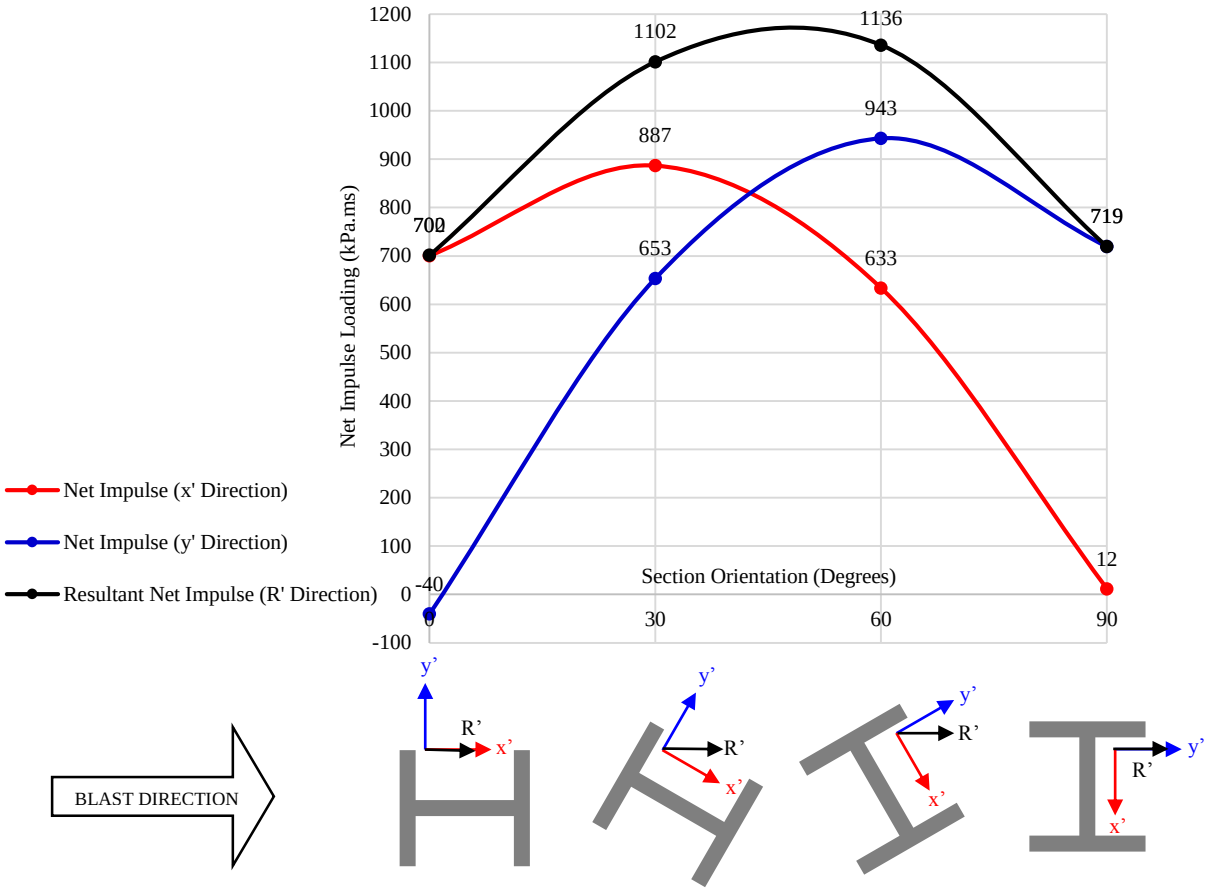

Figure 8: Calculated experimental net total impulse (component vectors and resultant) variation with I-section orientation.

Drag coefficients were calculated utilising the experimental pressure data, presented in Table 4 and plotted in Figure 9 with drag coefficients available in literature overlaid for comparison. Drag coefficients were generated by consideration of the net total impulse acting on the column in respective directions and the incident impulse associated with the dynamic pressures. The experimentally-derived drag coefficients (plotted by solid curves in Figure 9) intuitively exhibit a similar pattern to the net impulse plots. Unlike the net impulse curves however, a noticeable degree of skew is observed whereby the 60° orientation exhibits a more pronounced increase in drag coefficient, thus suggesting that the multi-axis blast loading of an I-section does not exhibit perfectly symmetrical behaviour.

Table 4: Experimentally-calculated drag coefficients.

Section Orientation	Experimentally-Calculated Drag Coefficients		
	$C_{D,x'}$	$C_{D,y'}$	$C_{D,R'}$
0°	1.6	0.0	1.6
30°	1.8	1.3	2.3
60°	1.4	2.1	2.5
90°	0.0	1.5	1.5

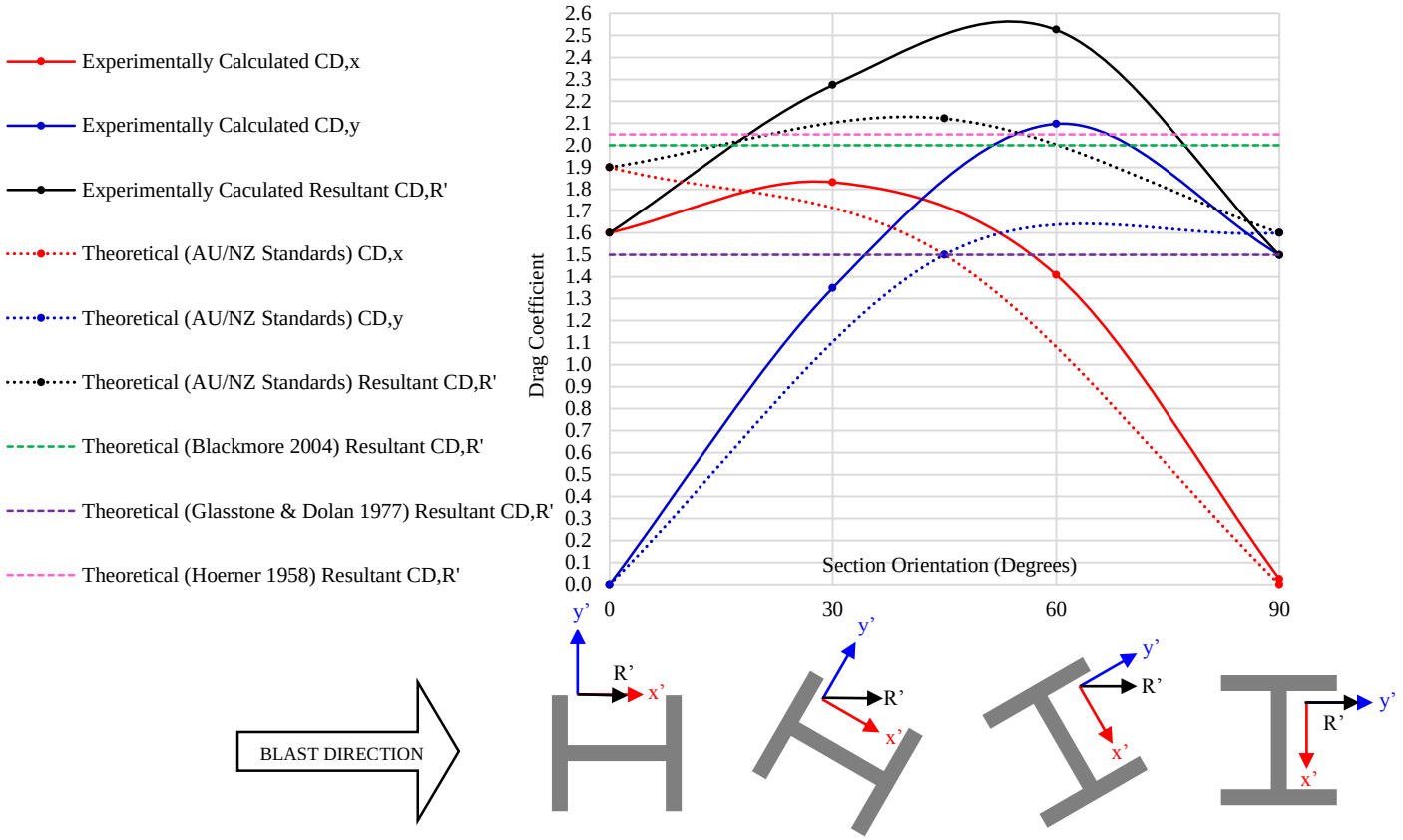

Figure 9: Calculated drag force coefficients and proposed blast and wind drag coefficients for different I-section orientations.

As part of this study, experimentally-derived drag coefficients are compared to values available in blast and wind design literature to verify their accuracy and applicability to I-sections subjected to multi-axis blast loading. The Australian/New Zealand Standards for Wind Actions [8] provide drag force coefficients in the x- and y-axes for an I-section geometry exposed to wind at orientations of 0, 45 and 90 degrees. Generally, these values demonstrate good agreement with the experimentally derived drag coefficients in terms of capturing the variation with section orientation (Figure 9). For the orthogonal interaction (0 and 90 degrees), the AU/NZ Wind Standards provide conservative values, slightly exceeding the drag coefficients calculated from the experimental data (Figure 9). For intermediate orientations however, drag coefficient values proposed by the AU/NZ standards fall below those derived from the experimental results and are therefore no longer reliable. Most notably, an extrapolated y' drag coefficient of $C_{D,y'}$ =1.65 for a 60° orientation based on the AU/NZ standards is far less than the experimentally-derived value of 2.1, representing an under prediction of 28%. This also disagrees with the AU/NZ standard's implication that a maximum drag coefficient in the y-direction occurs for a 90° orientation. Consequently, the AU/NZ standards fail to capture the relatively high drag force coefficients experienced for intermediate, oblique orientations. This confirms that knowledge of the intermediate, oblique angle interaction is important for accurately predicting the correct magnitude of blast loading.

The prevalence of blast drag coefficients pertinent to I-sections in literature is limited, particularly when considering varying section orientation or 'angle of attack'. Typically, single value drag coefficients are proposed, such as Glasstone and Dolan [9] or Hoerner [10] who suggest a value of C_D=1.5 and C_D=2.05 respectively for 'sharp edged sections'. Blackmore [11] suggests a value of

C_D=2.0 for all common sharp edged channel sections including I-sections. These proposed blast drag coefficients are overlaid in Figure 9 for comparison, although no guidance as to their applicability about different section axes is provided and are therefore assumed to remain constant throughout the orientations tested. The drag coefficient proposed by Glasstone & Dolan [9] C_D=1.5 under-predicts the experimentally-derived coefficients for all orientations tested, thus providing an unreliable prediction (Figure 9). For the 0, 30 and 90 degree orientations, it can be seen that the drag coefficients proposed by Hoerner [10] and Blackmore [11] are conservative, being sufficiently greater than the respective x' or y' drag coefficients calculated from the experimental data. For the 60° orientation however, the experimental y' drag coefficient ($C_{D,y'}$=2.1) exceeds all proposed values. This observation provides reason to question the degree of conservatism and validity of existing drag coefficients when oblique interaction is concerned. Moreover, proposed single value drag coefficients are intended to calculate drag loading in the direction of the blast flow i.e. the resultant translational loading effect on the column specimen. However, the calculated experimental resultant drag coefficients (which express the overall translational drag load resulting from both the x' and y' component directions) far exceed even the highest values in literature for intermediate section orientations (Figure 9). This again suggests that blast drag coefficients in literature are only conservative when orthogonal axis interaction is concerned (i.e. 0° or 90°). In summary, the proposed drag coefficients in literature tend to under-predict the values calculated from the experimental results for intermediate, oblique section orientations.

CONCLUSION

The effects of multi-axis, long-duration blast loading on I-sections and the associated drag force coefficients were previously unknown. Four long-duration blast experiments investigated the effects of I-section orientation with respect to blast propagation on the net blast loading and to assess the suitability and accuracy of proposed drag coefficients. Successful data capture of specific surface impulses recorded as a function of section orientation quantified the multi-axis blast interaction and aerodynamic effects. Variation of surface impulse with section orientation was seen to be influenced by the relative exposure of the surface to the blast and the presence of aerodynamic effects; flow separation, regions of wake and vorticity reduced the impulse transferred to less-exposed or entirely shielded surfaces. It was found that oblique section orientations generated larger net impulse on the column. Net translational impulse components acting on the section as a function of orientation were calculated with a maximum value observed for the 60° orientation.

Experimental drag force coefficients were calculated for the I-section as a function of the orientations tested and compared to blast drag coefficients available in literature and those from wind design standards. In general, proposed drag coefficients for I-sections generally under-predict the experimentally-derived values for oblique orientations, especially when considering the resultant effect. Most notably, the 60° orientation exhibited the highest drag coefficient ($C_{D,y'}$=2.1) exceeding even the most conservative proposed values. These results provide reason to question the accuracy of drag coefficients in literature for blast drag problems when oblique-axis interaction is concerned. This paper provides experimental results to inform engineers and researchers towards selecting appropriate drag coefficients for accurate calculation of translational blast drag loads acting on I-sections about different axes.

ACKNOWLEGEMENTS

The authors would like to express gratitude to Dr J. Severn and Mr B. Fry for their valuable support throughout this research. The assistance of Mr C. Tilbury is gratefully acknowledged for his support during the preparation and interpretation of experimental trials. Experimental results reported in this paper were obtained on MOD facilities. Permission to use these results is gratefully acknowledged.

REFERENCES

[1] Steel Construction Institute, "Buncefield Explosion Mechanism Phase 1 (Volumes 1 and 2)," Ascot, 2009.
[2] US Department of Defense (DoD), "UFC 3-340-02, 'Structures To Resist The Effects Of Accidental Explosions,'" Washington, D.C., 2008.
[3] H. L. Brode, "A Review of Nuclear Explosion Phenomena Pertinent to Protective Construction (R-425-PR)," Santa Monica, California, 1964.
[4] G. J. Ballantyne, A. S. Whittaker, M. Asce, G. F. Dargush, and A. J. Aref, "Air-Blast Effects on Structural Shapes of Finite Width," *J. Struct. Eng.*, vol. 136, no. February, pp. 152–159, 2010.
[5] P. D. Smith and J. G. Hetherington, *Blast and Ballistic Loading of Structures*. 1994.
[6] G. Mays and P. Smith, *Blast effects on buildings*, First Edit. Thomas Telford Limited, 1995.
[7] T. Krauthammer, *Modern Protective Structures*. 2008.
[8] Standards Australia Limited/Standards New Zealand, "AS-NZS 1170.2:2011, 'Structural Design Actions - Part 2 : Wind actions,'" 2011.
[9] S. Glasstone and P. J. Dolan, *The Effects of Nuclear Weapons*, Third Edit. United States Department Of Defense and the Energy Research and Development Administration, 1977.
[10] S. F. Hoerner, *Fluid Dynamic Drag*. 1958.
[11] P. Blackmore, *Wind loads on unclad structures (BRE)*. BRE Electronic Publications, 2004.